Available online at www.sciencedirect.com

ScienceDirect

Ceramics International 40 (2014) 3325–3331

CERAMICS INTERNATIONAL

www.elsevier.com/locate/ceramint

Synthesis, characterization and electrochemical performances of MoO_2 and carbon co-coated $LiFePO_4$ cathode materials

Shuxin Liu[a,b,*], Hengbo Yin[a], Haibin Wang[b], Jichuan He[b], Hong Wang[b]

[a]School of Material Science and Engineering, Jiangsu University, Zhenjiang 212013, Jiangsu, PR China
[b]School of Chemistry and Chemical Engineering, Mianyang Normal University, Mianyang 621000, Sichuan, PR China

Received 7 June 2013; received in revised form 23 September 2013; accepted 23 September 2013
Available online 29 September 2013

Abstract

The MoO_2 and carbon co-coated $LiFePO_4$ cathode materials were synthesized by a combined technique of solid state synthesis and the sol–gel method. Phase compositions and microstructures of the products were characterized by X-ray powder diffraction (XRD), Raman, SEM and TEM. Results indicate that MoO_2 can sufficiently coat on the $LiFePO_4$ surface and does not alter $LiFePO_4$ crystal structure, and the existence of MoO_2 increases the graphitization degree of carbon. SEM and TEM images reveal that MoO_2 presence has little impact on $LiFePO_4$ particle size. The electrochemical behavior of cathode materials was analyzed using galvanostatic measurement and cyclic voltammetry (CV). The results show that the existence of MoO_2 improves electrochemical performance of $LiFePO_4$ cathode material in specific capability and low-temperature behavior. The apparent lithium ion diffusion coefficient increases with MoO_2 content and maximizes around the MoO_2 content of $x=5$ wt%. It has been had further proved that the higher electronic conductivity of MoO_2 and carbon enhances the lithium ion transport to improve the electrochemical performance of $LiFePO_4$ cathode materials.

Keywords: B. Composites; B. Surfaces; C. Electrical conductivity; E. Batteries; $LiFePO_4$

1. Introduction

Lithium-ion batteries are regarded as the most advanced energy storage systems, which have been widely used in electric vehicles (EVs), hybrid electric vehicles (HEVs), dispersed energy storage systems, and so on. Since the olivine-type lithium iron phosphate ($LiFePO_4$) was reported by Padhi et al. in 1997 [1], it has received much attention as a promising storage compound for cathodes in lithium-ion batteries due to $LiFePO_4$ has high theoretical specific capacity (about 170 mAh g^{-1}), low costs, environmental friendliness and safety [2–4]. In addition, $LiFePO_4$ presents good cycle stability owning to its structural similarity in the charged and discharged states [5].

However, $LiFePO_4$ shows poor electronic conductivity and low lithium ion diffusivity, which are an obstacle when applied in high power batteries [1,6]. In order to overcome these problems, all kinds of methods have been proposed including carbon-coating on $LiFePO_4$ surface [7–10], cation doping [11–15] and particle size minimization [16–18]. Wherein, the carbon-coating and particles size minimization can improve the electrochemical performances of $LiFePO_4$ due to the increasing electronic conductivity and shortening diffusion length of lithium ions, respectively, however, the carbon addition and small particles size will reduce tap density and energy density [19]. Recently, some new methods have been explored to enhance electrochemical performances of $LiFePO_4$, such as oxide coated or modified $LiFePO_4$/C composites. Li et al. [20] proposed that SiO_2 coated $LiFePO_4$/C effectively enhanced the cycling capacity and reduced capacity fading at high temperature and alleviated the cell impedance. Liu et al. reported that the electrochemical lithium-ion deintercalation–intercalation processes of CeO_2 modified $LiFePO_4$ electrodes were improved compared to the pristine

---

*Corresponding author at: Mianyang Normal University, School of chemistry and Chemical Engineering, No.30, Section 1, Xianren Road, Mianyang, Sichuan, China, 621000. Tel.: +86 816 2200064; fax: +86 816 2200819.
E-mail address: liushuxin88@126.com (S. Liu).

http://dx.doi.org/10.1016/j.ceramint.2013.09.102

$LiFePO_4$ electrode [21]. CuO and carbon co-coated $LiFePO_4$ was reported by Cui et al. [22], the study found that the co-coating reduced the capacity fading and the interfacial resistances and the polarization of the cathode. Jin et al. reported that V_2O_3 modified $LiFePO_4$/C materials exhibited improved electrochemical performance both in rate capability and low-temperature behavior, and the presence of V_2O_3 improved the apparent lithium ion diffusion coefficient of $LiFePO_4$/C [23].

After review on the existing literatures, it can be found that oxide coating or modifying can improve the electrochemical performances of $LiFePO_4$ in cycling capacity, capacity fading, cell impedance, polarization and apparent lithium ion diffusion coefficient, and so on. But, most of oxides are electrochemical inactive metal oxide or semiconductor oxide with lower electronic conductivities in these literatures. In this paper, we have attempted to synthesize MoO_2 and carbon co-coated $LiFePO_4$ cathode materials by a combined technique of solid state synthesis and the sol–gel method. MoO_2 possesses high electrical conductivity [24], therefore, it is interesting to investigate the influence of MoO_2 and carbon co-coating on the electrochemical performance of $LiFePO_4$ cathode materials.

2. Experimental

2.1. Synthesis

$LiFePO_4$ cathode materials were prepared by solid phase synthesis process. The starting materials were ammonium dihydrogen phosphate ($NH_4H_2PO_4$, A.R.), iron oxalate dehydrate ($FeC_2O_4 \cdot 2H_2O$, A.R.), and lithium carbonate (Li_2CO_3, A.R.). Firstly, all the starting materials were dispersed into ethanol and then ball milled for 4 h. The mixture was initially dried at 80 °C, hand grinded with an agate mortar, and treated at 350 °C for 6 h, then calcined at 700 °C for 24 h in a tube furnace under flow purified N_2 atmosphere with the heating rate of $5\ ^\circ C\ min^{-1}$. After the tube furnace is cooled to room temperature, $LiFePO_4$ was obtained and was defined as sample F, it was used as a raw material for MoO_2 and carbon co-coated $LiFePO_4$ cathode materials. The MoO_2 and carbon co-coated $LiFePO_4$ cathode materials were synthesized by a sol–gel method. Firstly, ammonium molybdate ($(NH_4)_6Mo_7O_{24} \cdot 4H_2O$, A.R.) and citric acid ($C_6H_8O_7 \cdot H_2O$, A.R., 10 wt% of sample F mass) were dissolved into distilled water, then added $LiFePO_4$ (sample F). Then the slurry was stirred for 1 h and dried at 80 °C. Finally, the dried precursors were treated at 350 °C for 3 h then was heated to 600 °C for 6 h in a purified N_2 gas flow and the MoO_2 and carbon co-coated $LiFePO_4$ cathode materials (MoO_2 content is 0 wt%, 1 wt%, 3 wt%, 5 wt% and 10 wt%) were obtained. The obtained products were defined as sample A, B, C, D and E, respectively.

2.2. Characterization and electrochemical measurements

Structural analysis was carried out using X-ray diffraction (XRD, X'Pert PRO, CuKα radiation) and Raman spectroscopy (Raman, InVia, wavelength is 514.5 nm). The morphology and microstructure of the MoO_2 and carbon co-coated $LiFePO_4$ cathode materials were observed with a scanning electron microscope (SEM, FEI Quanta 200F) and a transmission electron microscope (TEM, JEM-2100).

Coin cells of the 2430 configuration were assembled in an argon-filled glove box. The cathode was prepared by mixing 80 wt% MoO_2 and carbon co-coated $LiFePO_4$ powder with 10 wt% conductive carbon black and 10 wt% polyvinylidene fluoride (PVDF) in a n-methyl-2-pyrrolidone (NMP) solution, which was then coated onto aluminum foil current collector and dried at 115 °C for 12 h in a vacuum drying oven. Lithium metal was used as the anode and a 1 M solution of $LiPF_6$ in EC: DEC (1:1, v/v) was used as the electrolyte with a microporous polypropylene sheet (Celgard 2320) as the separator. The cells were charged and discharged galvanostatically between 2.5 V and 4.2 V (vs. Li/Li^+) using a battery test system (LAND CT2001A). The cyclic voltammetry (CV) curves were obtained between the ranges of 2.5–4.2 V on an electrochemical work station (CHI 660E).

3. Results and discussion

3.1. Phase composition and morphology

Fig. 1 shows the X-ray diffraction patterns (XRD) of MoO_2 and carbon co-coated $LiFePO_4$ cathode materials. It can be seen that the main phase in these samples is orthorhombic $LiFePO_4$ with a space group of Pmna, and there is no evidence of diffraction peaks for MoO_2 and carbon due to their amorphous structure and/or low content in samples A, B, C and D. With the content of MoO_2 increasing, the diffraction peaks of MoO_2 are detected in sample E. The formation of MoO_2 must be from the decomposition of $(NH_4)_6Mo_7O_{24} \cdot 4H_2O$ and the carbothermal reduction from Mo^{6+} to Mo^{4+}. Because the sensitivity of XRD analysis is finite, MoO_2 is likely present in samples B, C and D. In addition, no impurities such as Fe_2P, Li_3PO_4 and others are

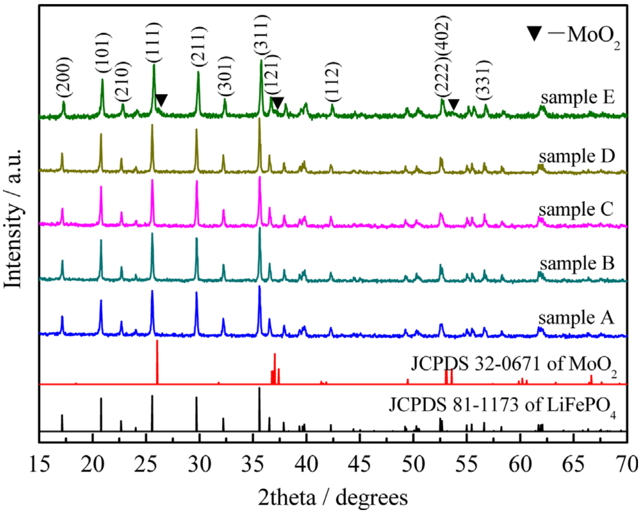

Fig. 1. XRD patterns of the MoO_2 and carbon co-coated $LiFePO_4$ cathode materials.

observed. All diffraction peaks are narrow, indicating that the $LiFePO_4$ grains are high crystallinity.

The carbon structure is closely related to the graphitization degree. In order to study the conductive carbon structure of the MoO_2 and carbon co-coated $LiFePO_4$ cathode materials, the Raman spectra test was carried out. Fig. 2 shows the Raman spectra of the samples A, B and D, respectively. All Raman spectra consist of two broad bands at 1350 and 1600 cm^{-1}, which can be ascribed to the characteristic Raman spectra of carbon coated layer. The bands at 1600 cm^{-1} mainly correspond to graphitized structured carbon of G band, while that at 1350 cm^{-1} corresponds to disordered structured carbon of D band [25,26]. The graphitized carbon contains sp^2 hybrid bonding, which is positively correlated with the electronic conductivity of carbon, and the disordered carbon mainly corresponds to sp^3 hybrid bonding. According to Doeff et al. [25,27,28] and Jin et al. [23] reports, the Raman spectra contain four overlapping absorption bands in range of 1100–1800 cm^{-1}. In order to get better results, the Raman spectra were processed by four Gaussian bands fitting. Those bands are located at 1220, 1350, 1510 and 1595 cm^{-1}, respectively. The bands at 1350 and 1595 cm^{-1} can be assigned to sp^2-type structure, and the others to sp^3-type. The integrated intensity ratios of sp^2/sp^3 $\left(I_{sp^2}/I_{sp^3}\right)$ of MoO_2 and carbon co-coated $LiFePO_4$ cathode materials (sample A, B, C, D and E) are 1.03, 1.13, 1.27, 1.52 and 1.53, respectively (Fig. 2(d)), it indicates that the graphitization degree of carbon increases with the MoO_2 content, and the carbon with higher graphitization degree can lead to the enhancement of electronic conductivity of $LiFePO_4$ cathode materials.

Fig. 3 shows the SEM and TEM images of sample A (Fig. 3(a)) and sample D (Fig. 3(b) and (c)). The SEM micrographs show that the particle size of samples A and D has very little difference, and sample D appears an aggregation to some extent. From comparison of samples A and D (Fig. 3(a) and (b)), we can find that the surface of sample D is rougher than sample A due to MoO_2 coating on the surface of $LiFePO_4$ particles. To further determine the existence of MoO_2 in cathode materials, sample D was analyzed by TEM (Fig. 3(c)). It can be seen that MoO_2 and carbon coat on the surface of $LiFePO_4$ particles and fill the interspaces between $LiFePO_4$ particles. The diameter of a $LiFePO_4$ grain is less than 1 μm, being consistent with the result of the SEM analysis (Fig. 3(b)). To further observe the structure of the MoO_2 and carbon layer, we magnify the selected square

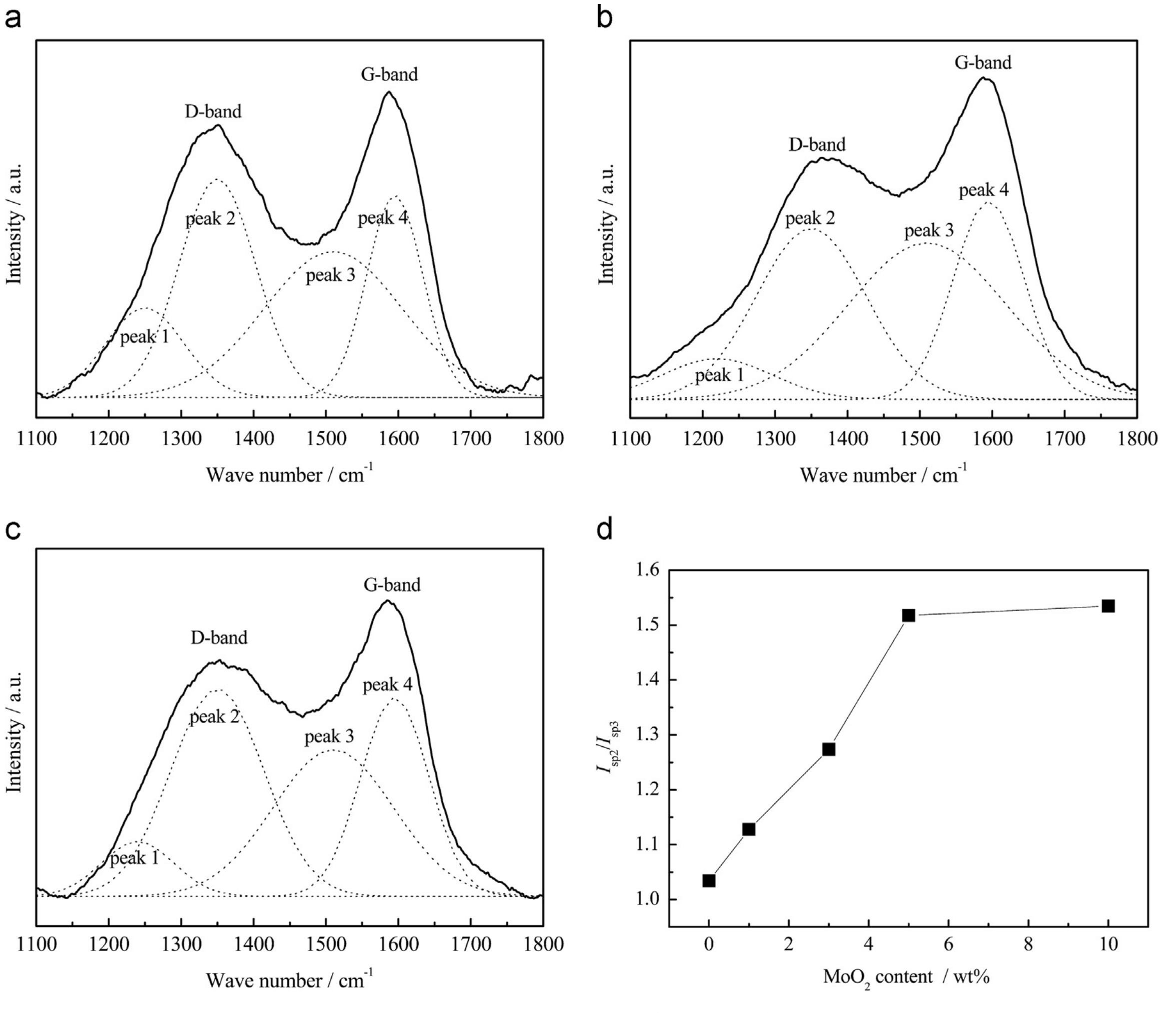

Fig. 2. Raman spectrum of sample A (a), sample B (b), sample D (c) (the dotted lines are from a Gaussian numerical simulation), and the relationship of $\left(I_{sp^2}/I_{sp^3}\right)$ vs. MoO_2 content (d).

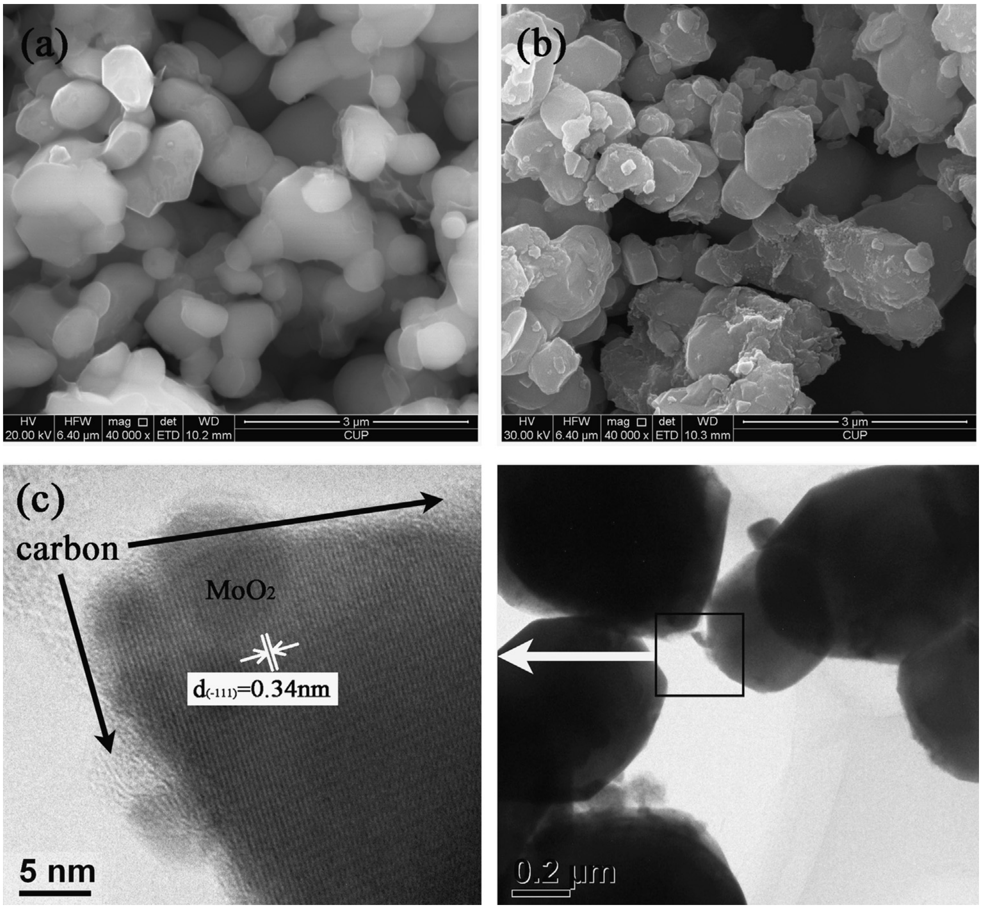

Fig. 3. SEM images of sample A (a) and sample D (b), and TEM image of sample D (c).

area in Fig. 3(c). In the well-crystallized area, the gaps between every two parallel stripes are measured to be 0.34 nm, which corresponds to the interplanar distance of (−1 1 1) planes of MoO_2 crystals. Meanwhile, there are many partially crystallized structure and disordered structure which are partly graphitized carbon. Hence, the surface of $LiFePO_4$ particles is actually coated by MoO_2 and carbon.

3.2. Electrochemical performance

Fig. 4 shows the charge–discharge curves at 0.1 C at room temperature for all samples. All the samples exhibit flat voltage plateaus around 3.5 V, which is the main characteristic of the two-phase reaction of the lithium extraction and insertion between $LiFePO_4$ and $FePO_4$ [29].The discharge specific capacities of samples (A, B, C, D and E) are 142.8, 145.2, 149.6, 153.2 and 148.5 mAh g^{-1}, respectively. Among them, the sample A has the least discharge specific capacity, and with increasing MoO_2 content, the samples B, C, D and E show higher specific capacity. In the synthesis process of MoO_2 and carbon co-coated $LiFePO_4$ cathode materials, Mo^{6+} is reduced to Mo^{4+} by carbon as reductant, so, the carbon content of cathode materials is decreasing with MoO_2 content increasing. It indicates that the increase MoO_2 in cathode materials can improve specific capacity because MoO_2 possesses much higher electrical conductivity. The sample D shows the highest discharge specific capacity of 153.2 mAh g^{-1}, and it is higher than CuO and carbon coated $LiFePO_4$/C composites [22] and V_2O_3 modified $LiFePO_4$/C composites [23]. However, the discharge specific capacity decreases when the amount of MoO_2 is too much, which is the case for sample E containing

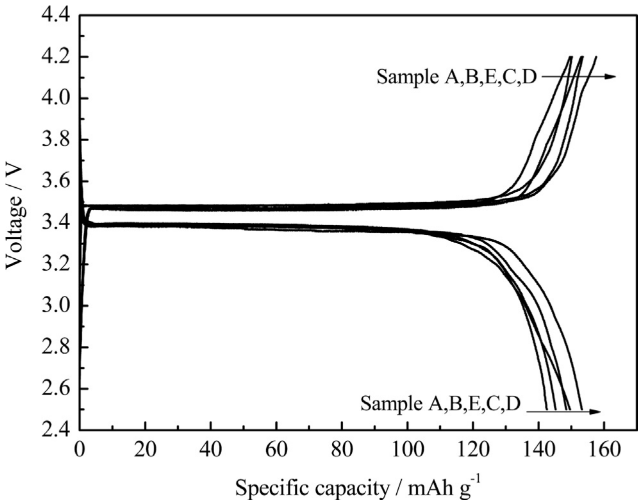

Fig. 4. Charge–discharge curves of the MoO_2 and carbon co-coated $LiFePO_4$ cathode materials at room temperature at 0.1 C.

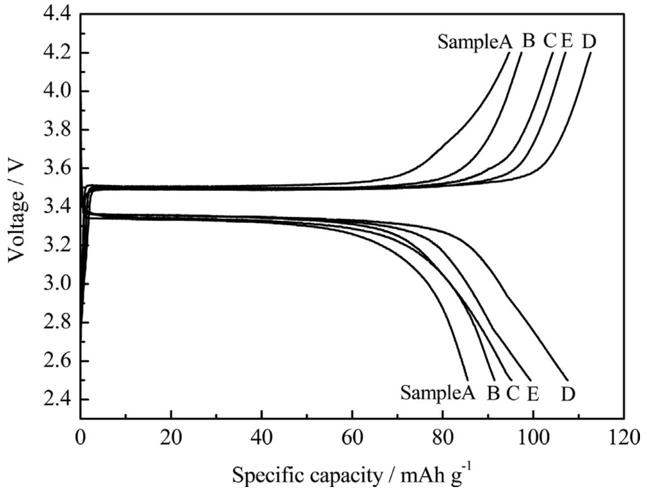

Fig. 5. Charge–discharge curves of the MoO_2 and carbon co-coated $LiFePO_4$ cathode materials at 0 °C at 0.1 C.

10 wt% MoO_2. The reason is that MoO_2 is inactive material, and too much inactive material will decrease specific capacity of cathode materials. Fig. 5 shows the charge–discharge curves of samples at 0.1 C at a low temperature of 0 °C. Compared with the room temperature performance, the voltage profiles vary a lot. Among five samples, sample D exhibits the highest discharge specific capacity (107.6 mAh g^{-1}) and the least polarization. Meanwhile, the sample A shows a rather poor performance with a low discharge specific capacity of 85.4 mAh g^{-1} and a larger polarization.

3.3. Apparent lithium ion diffusion coefficient

In order to study the apparent lithium ion diffusion coefficient in the MoO_2 and carbon co-coated $LiFePO_4$ cathode materials, the cyclic voltammetry (CV) was carried out at room temperature. Fig. 6(a) shows the CV of sample D in the voltage range of 2.5–4.2 V at scanning rates of 0.1, 0.2, 0.5 and 1.0 mV s^{-1}. It is obvious that the intensity and area of redox peaks increase with the scanning rate. Fig. 6(b) shows the relationship between the peak current and the scanning rate and it is found that the peak current has linear relationship with the square root of the scanning rate. So, the apparent lithium ion diffusion coefficient can be derived according to following Eq. :

$$i_{pc} = 0.4463(nF)^{3/2}(RT)^{-1/2}C_{Li^+}v^{1/2}AD_{Li^+}^{apparent1/2} \quad (1)$$

where, i_{pc} is the peak current (A), n is the charge-transfer number (one), F is the Faraday constant (96485.33 C mol^{-1}). R is the ideal gas constant (8.314 J mol^{-1} K^{-1}). T is the experimental temperature (298.15 K). C_{Li}^{+} is the concentration of Li-ion in the cathode (0.0228 mol cm^{-3}). v is the scanning rate (V s^{-1}). A is the contact area between $LiFePO_4$ and electrolyte (here A approximates the surface area of electrode, 1.54 cm^2) and $D_{Li^+}^{apparent}$ is the apparent lithium ion diffusion coefficients (cm^2 s^{-1}) [23,30].

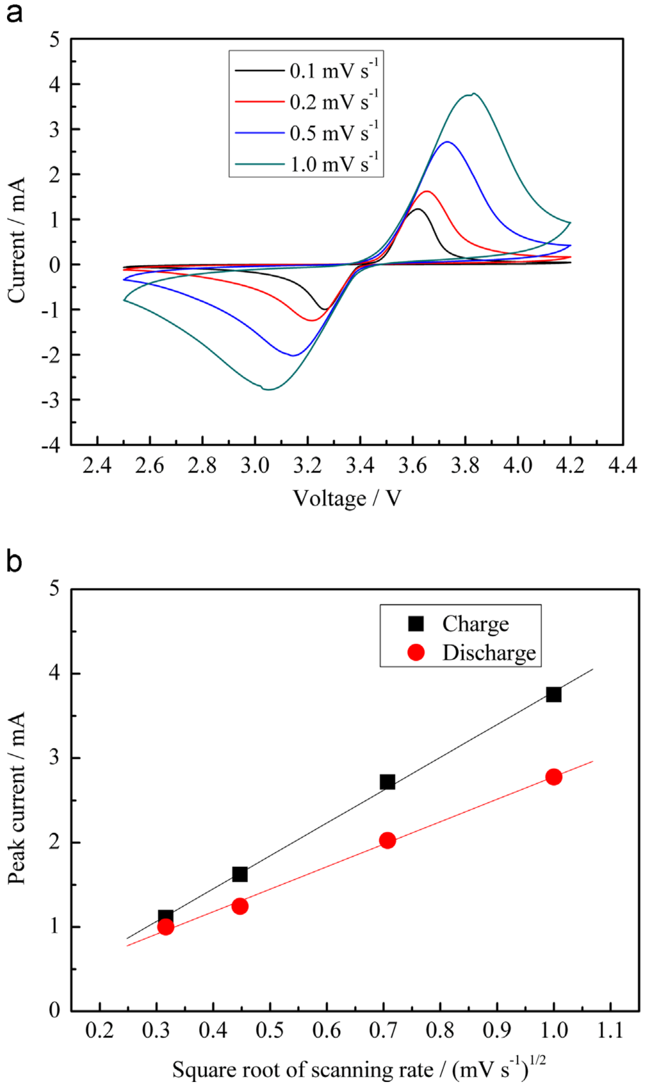

Fig. 6. Cyclic voltammetry of sample D in the voltage range of 2.5–4.2 V at scanning rates of 0.1, 0.2, 0.5 and 1.0 mV s^{-1} (a) and the relationship of peak current and the square root of the scanning rate (b).

Fig. 7(a) shows the CV of sample A, B, C, D and E in the voltage range of 2.5–4.2 V at scanning rates of 0.1 mV s^{-1} and the peak currents of samples are 0.6628, 0.6897, 1.1593, 1.2291 and 0.9375 mA respectively, during charge, and 0.5660, 0.5671, 0.9209, 0.9976 and 0.7330 mA, respectively, during discharge. We can use these data to calculate the apparent lithium ion diffusion coefficient of samples by Eq. (1). The variation of the apparent lithium ion diffusion coefficient in the charge and discharge process is shown in Fig. 7(b). The values of the apparent lithium ion diffusion coefficient vary from 4.92×10^{-11} to 1.69×10^{-10} cm^2 s^{-1} during charge and from 3.59×10^{-11} to 1.12×10^{-10} cm^2 s^{-1} during discharge depending on the MoO_2 content. Sample D gives the highest value of 1.69×10^{-10} cm^2 s^{-1} during charge and 1.11×10^{-10} cm^2 s^{-1} during discharge, and they are higher than CeO_2 modified $LiFePO_4$/C composites [21] and V_2O_3 modified $LiFePO_4$/C composites [23] and ZnO incorporated $LiFePO_4$ cathode materials [31]. It is found that the apparent lithium ion diffusion coefficient in the charge process is slightly larger than in the discharge process, it is clarified

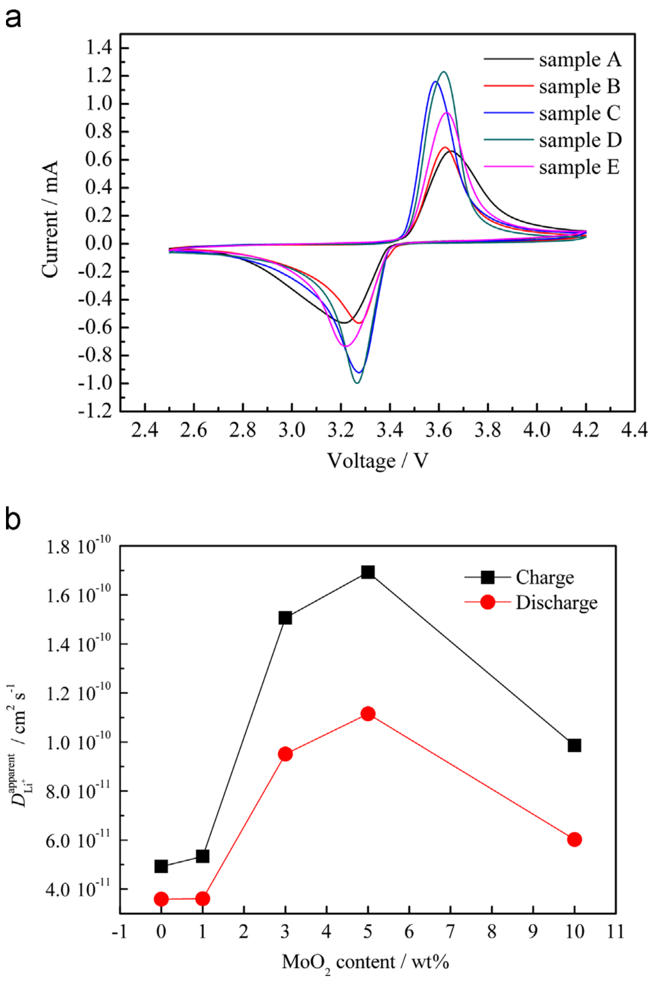

Fig. 7. Cyclic voltammetry of the MoO_2 and carbon co-coated $LiFePO_4$ cathode materials at a constant scanning rate of 0.1 mV s^{-1} (a) and the relationship of apparent lithium ion diffusion coefficient and MoO_2 content (b).

that the discharge process in $LiFePO_4$ is slower than the charge process. Meanwhile, it is found that the apparent lithium ion diffusion coefficient in both charge and discharge process increases with MoO_2 content, besides it takes a maximum $x=5$ wt%. So, the existence of MoO_2 can improve the ionic conduction in $LiFePO_4$ in both charge and discharge processes. It is also possible to explain the experimental facts about the improved electrochemical performance of the MoO_2 and carbon co-coated $LiFePO_4$ cathode materials from the viewpoint of the ionic conduction, which was shown in Figs. 4 and 5.

4. Conclusions

To improve the electrical conductivity and lithium ion diffusivity of $LiFePO_4$ cathode materials, the MoO_2 and carbon co-coated $LiFePO_4$ cathode materials were synthesized by a combined technique of solid state synthesis and sol–gel methods. The existence of MoO_2 as a conductive oxide improves the electronic conductivity of $LiFePO_4$ cathode materials and decreases polarization of electrode. Meanwhile, the presence of MoO_2 increases the graphitization degree of carbon to improve the electronic conductivity of $LiFePO_4$ cathode materials. Charge–discharge and cyclic voltammetry tests show that the existence of MoO_2 improves electrochemical performance of $LiFePO_4$ cathode materials in specific capability and low-temperature behavior. Meanwhile, the existence of MoO_2 affects the ionic diffusion during both the charge and discharge processes. The apparent lithium ion diffusion coefficient increases with MoO_2 content and maximizes around the MoO_2 content of $x=5$ wt%. So, the existence of MoO_2 enhances both electronic and ionic conductivities.

Acknowledgments

This work was supported by the Applied Basic Research Project of Sichuan Province (2011JY0101), the Key Fund Project of Sichuan Education Department (13ZA0111), the Natural Science Fund Project of Sichuan Education Department (11ZB239), the Science and Technology Research Project of Mianyang (12G031-1) and the Key Project of Mianyang Normal University (2012A11).

References

[1] A.K. Padhi, K.S. Nanjundaswamy, J.B. Goodenough, Phospho-olivines as positive-electrode materials for rechargeable lithium batteries, Journal of the Electrochemical Society 144 (1997) 1188–1194.

[2] J.K. Kim, G. Cheruvally, J.W. Choi, J.U. Kim, J.H. Ahn, G.B. Cho, K.W. Kim, H.J. Ahn, Effect of mechanical activation process parameters on the properties of $LiFePO_4$ cathode material, Journal of Power Sources 166 (2007) 211–218.

[3] G. Arnold, J. Garche, R. Hemmer, S. Ströbele, C. Vogler, M. Wohlfahrt-Mehrens, Fine-particle lithium iron phosphate $LiFePO_4$ synthesized by a new low-cost aqueous precipitation technique, Journal of Power Sources 119/121 (2003) 247–251.

[4] M. Takahashi, H. Ohtsuka, K. Akuto, Y. Sakurai, Confirmation of long-term cyclability and high thermal stability of $LiFePO_4$ in prismatic lithium-ion cells, Journal of the Electrochemical Society 152 (2005) A899–A904.

[5] H. Huang, S.C. Yin, L.F. Nazar, Approaching theoretical capacity of $LiFePO_4$ at room temperature at high rates, Electrochemical and Solid-State Letters 4 (2001) A170–A172.

[6] B. Kang, G. Ceder, Battery materials for ultrafast charging and discharging, Nature 458 (2009) 190–193.

[7] X. Zhi, G. Liang, L. Wang, X. Ou, L. Gao, X. Jie, Optimization of carbon coatings on $LiFePO_4$: carbonization temperature and carbon content, Journal of Alloys and Compounds 503 (2010) 370–374.

[8] K. Kim, Y.H. Cho, D. Kam, H.S. Kim, J.W. Lee, Effects of organic acids as reducing agents in the synthesis of $LiFePO_4$, Journal of Alloys and Compounds 504 (2010) 166–170.

[9] N. Ravet, Y. Chouinard, J.F. Magnan, S. Besner, M. Gauthier, M. Armand, Electroactivity of natural and synthetic triphylite, Journal Power Sources 97–98 (2001) 503–507.

[10] K. Yang, Z.H. Deng, J.S. Suo, Effects of carbon sources and carbon contents on the electrochemical properties of $LiFePO_4$/C cathode material, Journal of Solid State Electrochemistry 16 (2012) 2805–2813.

[11] L. Wu, X. Li, Z. Wang, H. Guo, X. Wang, F. Wu, J. Fang, Z. Wang, L. Li, A novel process for producing synthetic rutile and $LiFePO_4$ cathode material from ilmenite, Journal of Alloys and Compounds 506 (2010) 271–278.

[12] D. Arumugam, G. Paruthimal Kalaignan, P. Manisankar, Synthesis and electrochemical characterizations of nano-crystalline $LiFePO_4$ and Mg-doped

$LiFePO_4$ cathode materials for rechargeable lithium-ion batteries, Journal. of Solid State Electrochemistry 13 (2009) 301–307.

[13] J. Yao, K. Konstantinov, G.X. Wang, H.K. Liu, Electrochemical and magnetic characterization of $LiFePO_4$ and $Li_{0.95}Mg_{0.05}FePO_4$ cathode materials, Journal of Solid State Electrochemistry 11 (2007) 177–185.

[14] N. Hua, C. Wang, X. Kang, T. Wumair, Y. Han, Studies of V doping for the $LiFePO_4$-based Li ion batteries, Journal of Alloys and Compounds 503 (2010) 204–208.

[15] X.S. Fang, J. Li, K.L. Huang, S.Q. Liu, C.H. Huang, S.X. Zhuang, J.B. Zhang, Synthesis of nano-$LiFePO_4$ particles with excellent electrochemical performance by electrospinning-assisted method, Journal of Solid State Electrochemistry 16 (2012) 767–773.

[16] D.H. Kim, J. Kim, Synthesis of $LiFePO_4$ nanoparticles in polyol medium and their electrochemical properties, Electrochemical and Solid-State Letters 9 (2006) A439–A442.

[17] S.B. Lee, I.C. Jang, H.H. Lim, V. Aravindan, H.S. Kim, Y.S. Lee, Preparation and electrochemical characterization of $LiFePO_4$ nanoparticles with high rate capability by a sol–gel method, Journal of Alloys Compounds 491 (2010) 668–672.

[18] M.J. Li, L.Q. Sun, K. Sun, S.H. Yu, R.S. Wang, H.M. Xie, Synthesis of nano-$LiFePO_4$ particles with excellent electrochemical performance by electrospinning-assisted method, Journal of Solid State Electrochemistry 16 (2012) 3581–3586.

[19] Z.H. Chen, J.R. Dahn, Reducing carbon in $LiFePO_4$/C composite electrodes to maximize specific energy, volumetric energy, and tap density, Journal of the Electrochemical Society 149 (2002) A1184–A1189.

[20] Y. Li, S. Zhao, C. Nan, B.H. Li, Electrochemical performance of SiO_2-coated $LiFePO_4$ cathode materials for lithium ion battery, Journal of Alloys and Compounds 509 (2011) 957–960.

[21] Y. Liu, C. Mi, C. Yuan, X. Zhang, Improvement of electrochemical and thermal stability of $LiFePO_4$ cathode modified by CeO_2, Journal of Electroanalytical Chemistry 628 (2009) 73–80.

[22] Y. Cui, X. Zhao, R. Guo, Enhanced electrochemical properties of $LiFePO_4$ cathode material by CuO and carbon co-coating, Journal of Alloys and Compounds 490 (2010) 236–240.

[23] Y. Jin, C. Yang, X. Rui, T. Cheng, C. Chen, V_2O_3 modified $LiFePO_4$/C composite with improved electrochemical performance, Journal of Power Sources 196 (2011) 5623–5630.

[24] C.H. Guo, G.J. Zhang, Z.R. Shen, P.C. Sun, Z.Y. Yuan, Q.H. Jin, B.H. Li, D.T. Ding, T.H. Chen, Hydrothermal synthesis and formation mechanism of mircrometer-sized MoO_2 hollow spheres, Chinese Journal of Chemical Physics 19 (2006) 543–549.

[25] M.M. Doeff, J.D. Wilcox, R. Kostecki, G. Lau, Optimization of carbon coatings on $LiFePO_4$, Journal of Power Sources 163 (2006) 180–184.

[26] T. Nakamura, Y. Miwa, M. Tabuchi, Y. Yamada, Structural and surface modifications of $LiFePO_4$ olivine particles and their electrochemical properties, Journal of the Electrochemical Society 153 (2006) A1108–A1114.

[27] M.M. Doeff, Y. Hu, F. McLarnon, R. Kostecki, Effect of surface carbon structure on the electrochemical performance of $LiFePO_4$, Electrochemical and Solid-State Letters 6 (2003) A207–A209.

[28] Y. Hu, M.M. Doeff, R. Kostecki, R. Finones, Electrochemical performance of sol–gel synthesized $LiFePO_4$ in lithium batteries, Journal of the Electrochemical Society 151 (2004) A1279–A1285.

[29] M. Takahashi, S. Tobishima, K. Takei, Y. Sakurai, Characterization of $LiFePO_4$ as the cathode material for rechargeable lithium batteries, Journal of Power Sources 97 (2001) 508–511.

[30] P.P. Prosini, M. Lisi, D. Zane, M. Pasquali, Determination of the chemical diffusion coefficient of lithium in $LiFePO_4$, Solid State Ionics 148 (2002) 45–51.

[31] J. Lee, P. Kumar, J. Lee, B.M. Moudgil, R.K. Singh, ZnO incorporated $LiFePO_4$ for high rate electrochemical performance in lithium ion rechargeable batteries, Journal of Alloys and Compounds 550 (2013) 536–544.